Ultrafast optical switching in quantum dot-metallic nanoparticle hybrid systems

Wen-Xing Yang,[1,2,*] **Ai-Xi Chen,**[3,4] **Ziwen Huang,**[1] **and Ray-Kuang Lee**[2]

[1]*Department of Physics, Southeast University, Nanjing 210096, China*
[2]*Institute of Photonics Technologies, National Tsing-Hua University, Hsinchu 300, Taiwan*
[3]*Department of Applied Physics, School of Basic Science, East China Jiaotong University, Nanchang 330013, China*
[4]*Institute for Quantum Computing, University of Waterloo, Ontario N2L 3G1, Canada*
[*]*wenxingyang@seu.edu.cn*

Abstract: We study ultrafast excitonic population inversion resulting from the interaction of a semiconductor quantum dot (SQD) with localized surface plasmons. The plasmonic enhanced fields are generated when a metallic nanoparticle (MNP) is subject to a nonlinear chirped few-cycle pulse train. By numerically solving the time-dependent Bloch equations beyond the rotating-wave approximation, we show that the complete population inversion can be achieved for small interparticle distance and the dynamic in population inversion exhibits a steplike transition between absorption and amplifying. This phenomenon can be exploited as an all-optical ultrafast switching device. Moreover, the final state of population inversion is shown to be modified significantly with the interparticle distances, which is not only robust against the variation of probe pulse parameters but also suggests a straightforward method for measuring the interparticle distances via probing the final populations.

© 2015 Optical Society of America

OCIS codes: (320.7130) Ultrafast processes in condensed matter, including semiconductors; (270.1670) Coherent optical effects; (240.6680) Surface plasmons.

References and links

1. W. Zhang, A.O. Govorov, and G.W. Bryant, "Semiconductor-metal nanoparticle molecules: hybrid excitons and the nonlinear Fano effect," Phys. Rev. Lett. **97**, 146804 (2006).
2. M.T. Cheng, S.D. Liu, H.J. Zhou, Z.H. Hao, and Q.Q. Wang, "Coherent exciton-plasmon interaction in the hybrid semiconductor quantum dot and metal nanoparticle complex," Opt. Lett. **32**, 2125–2127 (2007).
3. J.Y. Yan, W. Zhang, S.Q. Duan, X.G. Zhao, and A.O. Govorov, "Optical properties of coupled metal-semiconductor and metal-molecule nanocrystal complexes: Role of multipole effects," Phys. Rev. B **77**, 165301 (2008).
4. R.D. Artuso and G.W. Bryant, "Optical response of strongly coupled quantum dot-metal nanoparticle systems: double peaked Fano structure and bistability," Nano Lett. **8**, 2106–2111 (2008).
5. P. Vasa, R. Pomraenke, S. Schwieger, Yu.I. Mazur, Vas. Kunets, P. Srinivasan, E. Johnson, J.E. Kihm, D.S. Kim, E. Runge, G. Salamo, and C. Lienau, "Coherent exciton-surface-plasmon-polariton interaction in hybrid metal-semiconductor nanostructures, Phys. Rev. Lett. **101**, 116801 (2008).
6. S.M. Sadeghi, "Plasmonic metaresonances: molecular resonances in quantum dot-metallic nanoparticle conjugates," Phys. Rev. B **79**, 233309 (2009).
7. Z. Lu and K.D. Zhu, "Slow light in an artificial hybrid nanocrystal complex," J. Phys. B **42**, 015502 (2009).
8. S.M. Sadeghi, "Coherent control of metallic nanoparticles near fields: Nanopulse controllers and functional nanoamplifiers," Phys. Rev. B **82**, 035413 (2010).
9. A. Ridolfo, O.Di Stefano, N. Fina, R. Saija, and S. Savasta, "Quantum plasmonics with quantum dot-metal nanoparticle molecules: influence of the Fano effect on photon statistics," Phys. Rev. Lett. **105**, 263601 (2010).

#235144 - $15.00 USD Received 25 Feb 2015; revised 15 Apr 2015; accepted 3 May 2015; published 8 May 2015
© 2015 OSA

10. E. Waks and D. Sridharan, "Cavity QED treatment of interactions between a metal nanoparticle and a dipole emitter," Phys. Rev. A **82**, 043845 (2010).
11. A.O. Govorov, "Semiconductor-metal nanoparticle molecules in a magnetic field: Spin-plasmon and exciton-plasmon interactions," Phys. Rev. B **82**, 155322 (2010).
12. R.D. Artuso and G.W. Bryant, "Strongly coupled quantum dot-metal nanoparticle systems: Exciton-induced transparency, discontinuous response, and suppression as driven quantum oscillator effects," Phys. Rev. B **82**, 195419 (2010).
13. J.T. Zhang, Y. Tang, K. Lee, and M. Ouyang, "Tailoring light-matter-spin interactions in colloidal hetero-nanostructures," Nature (London) **466**, 91–95 (2010).
14. R.D. Artuso, G.W. Bryant, A. Garcia-Etxarri, and J. Aizpurua, "Using local fields to tailor hybrid quantum-dot/metal nanoparticle systems," Phys. Rev. B **83**, 235406 (2011).
15. A.V. Malyshev and V.A. Malyshev, "Optical bistability and hysteresis of a hybrid metal-semiconductor nanodimer," Phys. Rev. B **84**, 035314 (2011).
16. A. Hatef, D.G. Schindel, and M.R. Singh, "Dipole-dipole interaction in a quantum dot and metallic nanorod hybrid system," Appl. Phys. Lett. **99**, 181106 (2011).
17. M.L. Andersen, S. Stobbe, A.S. Sorensen, and P. Lodahl, "Strongly modified plasmonCmatter interaction with mesoscopic quantum emitters," Nat. Phys. **7**, 215–218 (2011).
18. N.T. Fofang, N.K. Grady, Z.Y. Fan, A.O. Govorov, and N.J. Halas, "Plexciton Dynamics: Exciton-Plasmon Coupling in a J-Aggregate?Au Nanoshell Complex Provides a Mechanism for Nonlinearity," Nano. Lett. **11**, 1556–1560 (2011).
19. M.T. Cheng, X.S. Ma, Y.Q. Luo, P.Z. Wang, and G.X. Zhao, "Entanglement generation and quantum state transfer between two quantum dot molecules mediated by quantum bus of plasmonic circuits," Appl. Phys. Lett. **99**, 223509 (2011).
20. J.B. Li, N.C. Kim, M.T. Cheng, L. Zhou, Z.H. Hao, and Q.Q. Wang, "Optical bistability and nonlinearity of coherently coupled exciton-plasmon systems," Opt. Express **20**, 1856–1861 (2012).
21. M.A. Antón, F. Carreño, S. Melle, O.G. Calderón, E. Cabrera-Granado, J. Cox, and M. R. Singh, "Plasmonic effects in excitonic population transfer in a driven semiconductor-metal nanoparticle hybrid system," Phys. Rev. B **86**, 155305 (2012).
22. S.G. Kosionis, A.F. Terzis, S.M. Sadeghi, and E. Paspalakis, "Optical response of a quantum dot-metal nanoparticle hybrid interacting with a weak probe field," J. Phys.: Condens. Matter **25**, 045304 (2013).
23. S.M. Sadeghi, "Quantum coherence effects in hybrid nanoparticle molecules in the presence of ultra-short dephasing times," Appl. Phys. Lett. **101**, 213102 (2012).
24. E. Paspalakis, S. Evangelou, and A.F. Terzis, "Control of excitonic population inversion in a coupled semiconductor quantum dot-metal nanoparticle system," Phys. Rev. B **87**, 235302 (2013).
25. A. Hatef, S.M. Sadeghi, S. Fortin-Deschnes, E. Boulais, and M. Meunier, "Coherently-enabled environmental control of optics and energy transfer pathways of hybrid quantum dot-metallic nanoparticle systems," Opt. Express **21**, 5643–5653 (2013).
26. M.A. Antón, F. Carreño, S. Melle, O.G. Calderón, E. Cabrera-Granado, and M.R. Singh, "Optical pumping of a single hole spin in a p-doped quantum dot coupled to a metallic nanoparticle," Phys. Rev. B **87**, 195303 (2013).
27. P. Vasa, W. Wang, R. Pomraenke, M. Lammers, M. Maiuri, C. Manzoni, G. Cerullo, and C. Lienau, "Real-time observation of ultrafast Rabi oscillations between excitons and plasmons in metal nanostructures with J-aggregates," Nat. Photonics **7**, 128–132 (2013).
28. S.L. Sewall, A. Franceschetti, R.R. Cooney, A. Zunger, and P. Kambhampati, "Direct observation of the structure of band-edge biexcitons in colloidal semiconductor CdSe quantum dots," Phys. Rev. B **80**, 081310(R) (2009).
29. S.M. Sadeghi and R.G. West, "Coherent control of Forster energy transfer in nanoparticle molecules: energy nanogates and plasmonic heat pulses," J. Phys.: Condens. Matter **23**, 425302 (2011).
30. D.E. Chang, A.S. Sorensen, P.R. Hemmer, and M.D. Lukin, "Quantum Optics with Surface Plasmons," Phys. Rev. Lett. **97**, 053002 (2006).
31. A. Franceschetti, H. Fu, L.W. Wang, and A. Zunger, "Many-body pseudopotential theory of excitons in InP and CdSe quantum dots," Phys. Rev. B **60**, 1819–1829 (1999).
32. P.B. Johnson and R.W. Christy, "Optical Constants of the Noble Metals," Phys. Rev. B **6**, 4370–4379 (1972).
33. S.T. Cundiff and J. Ye, "Colloquium: Femtosecond optical frequency combs," Rev. Mod. Phys. **75**, 325–342 (2003).
34. M.O. Scully and M.S. Zubariry, "Quantum optics," (Cambridge University Press, 1997).
35. M.E. Crenshaw and C.M. Bowden, "Quasiadiabatic following approximation for a dense medium of two-level atoms," Phys. Rev. Lett. **69**, 3475–3478 (1992).
36. L. Allen and J.H. Eberly, *Optical Resonance and Two-Level Atoms* (Dover, Toronto, 1987).
37. A. Tcherniak, J.W. Ha, S. Dominguez-Medina, L.S. Slaughter, and S. Link, "Probing a century old prediction one plasmonic particle at a time," Nano Lett. **10**, 1398–1404 (2010).
38. L.J.E. Anderson, K.M. Mayer, R.D. Fraleigh, Y. Yang, S. Lee, and J.H. Hafner, "Quantitative measurements of individual gold nanoparticle scattering cross sections," J. Phys. Chem. C **114**, 11127–11132 (2010).
39. L.S. Slaughter, W.-S. Chang, P. Swanglap, A. Tcherniak, B.P. Khanal, E.R. Zubarev, and S. Link, "Single-particle

#235144 - $15.00 USD Received 25 Feb 2015; revised 15 Apr 2015; accepted 3 May 2015; published 8 May 2015
© 2015 OSA

spectroscopy of gold nanorods beyond the quasi-static limit: varying the width at constant aspect ratio," J. Phys. Chem. C **114**, 4934–4938 (2010).

There have been significant research activities on the hybrid systems consisting of one semiconductor quantum dot (SQD) and one metallic nanoparticle (MNP) for many potential applications [1–27]. When the exciton energy of a SQD is on resonance with the plasmon peak of the MNP, strong exciton-plasmon coupling can be observed on the power absorption in a SQD-MNP hybrid system [1, 11]. Coherent dynamics in excitons and optical properties of the hybrid complexes can be modified significantly by the strong coherent interaction [1–27]. Several fascinating effects induced through exciton-plasmon coherent couplings have been discovered when lasers are applied to these hybrid systems, such as controllable Rabi oscillations [2, 6], plasmonic metal-resonances [6], tunable ultrafast nanoswitches [8], modified resonance fluorescence and photon statistics [9, 10], creation of plasmonically induced transparency [22], controlling speed of light [7], and intrinsic bistability and hysteresis [4, 15, 20] in these hybrid complexes.

Controlled dynamics of exciton population inversion between the ground and single-exciton states has been analyzed in the SQD-MNP hybrid system [2, 5, 8, 21, 24], which showed that the population and Rabi oscillations in the SQD is significantly altered due to the presence of MNP. Specifically, the final population inversion induced by a widely used π pulse can be destroyed for small interparticle distances due to the interaction between excitons and surface plasmon [24]. One area of ongoing interest is the ultrafast optical switching mechanism for the exciton population inversion. Motivated by this, we study the optical switching in the population inversion between the ground and single-exciton states in a coupled system composed of a SQD and a MNP. We give an emphasis to the case of interaction of this hybrid system with electromagnetic pulses of few cycles in duration. We numerically solve the effective nonlinear Bloch equations for a hybrid complex consisting of a small SQD and a spherical MNP, by taking into account the ultrashort nature of the applied field. A complete population inversion is shown to be possible and the related population inversion dynamic exhibits a steplike transition between absorption and amplifying even for small interparticle distances. In addition, the final population inversion can be modified significantly by the interparticle distances, which might suggest a straightforward method for measuring the interparticle distances from the final state of the inversion. More importantly, the present results are reasonably robust with respect to pulse shape, electric field amplitude, and chirped parameter. Our study not only provides an efficient tool to manipulate the ultrafast dynamics of SQD system with wide adjustable parameters but also represents an achievement in this direction. Our results may also have potential applications in the development of ultrafast all-optical switching and solid-state quantum information science.

The hybrid system under consideration is illustrated in Fig. 1. The device is composed of a spherical MNP of radius a and a spherical SQD of radius b in the environment with dielectric constant ε_e. The center-to-center distance between the two particles is denoted as R. The parameters of the system, i.e., the size of the SQD and MNP, the center-to-center distance between two particles, are chosen such that the SQD has small dimensions $b \ll a$ and the size of the MNP is constraint as $a < R$. Here the SQD is characterized by a two-level system, with $|0\rangle$ being the ground state and $|1\rangle$ being the single-exciton state [3,12,28]. We will study the dynamics of this hybrid system driven by a linear polarization few-cycle chirped pulse train. The total electric field for the train of pulse can be written as $\vec{E}(t-nt_0) = \sum_{n=0}^{N-1} \hat{z}E_0 f(t)\cos[\omega(t)+\phi(t)]$. Here $\hat{z}$ is the polarization unit vector (along the z direction), E_0 is the electric field amplitude, $f(t)$ is the dimensionless pulse envelope, ω is the angular frequency, t_0 is the pulse repetition time, and $\phi(t)$ is the time-dependent phase of the applied field. The electric field excites both the inter-

#235144 - $15.00 USD Received 25 Feb 2015; revised 15 Apr 2015; accepted 3 May 2015; published 8 May 2015
© 2015 OSA

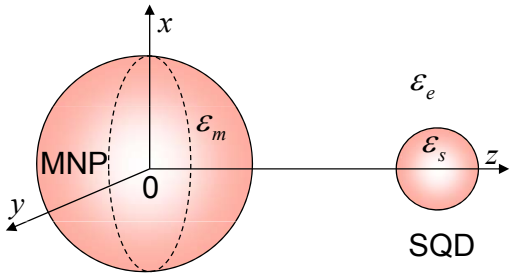

Fig. 1. Schematic diagram of our hybrid system composed of a semiconductor quantum dot (SQD) and a metallic nanoparticle (MNP). The centers of the two particles are separated by a distance represented by R.

band transition in the SQD and the surface plasmon in a MNP. Such surface plasmon influence the exciton and induce electromagnetic interactions between exciton and plasmon [1–3]. This interaction is responsible for the coupling between the two particles and leads to Förster energy transfer [29]. Under the dipole approximation, the Hamiltonian of the system can be written as,

$$H = \hbar\omega_{10} |1\rangle\langle 1| - \mu E_{SQD} (|0\rangle\langle 1| + |1\rangle\langle 0|), \tag{1}$$

where μ represents the dipole moment of the semiconductor quantum dot corresponding to the single-exciton transition, and E_{SQD} denote the total electric field inside the semiconductor quantum dot. To properly calculate E_{SQD}, we separate out the positive and negative frequency contributions as they exhibit different time responses. Thus E_{SQD} can be expressed as

$$E_{SQD}(t) = \frac{\hbar}{\mu}\left[\left(\frac{\Omega(t)}{2} + G\rho_{10}(t)\right) + \left(\frac{\Omega^*(t)}{2} + G^*\rho_{01}(t)\right)\right], \tag{2}$$

where $\rho_{ij}(t)$ is the density matrix elements. In Eq. (2), we defined the time-dependent Rabi frequency

$$\Omega(t) = (\Omega_0 + \Omega)\sum_{n=0}^{N-1} f(t) e^{-i[\omega(t-nt_0)+\phi(t)]} \tag{3}$$

with $\Omega = \frac{s_a\gamma_1 a^3}{R^3}\Omega_0 = \frac{s_a\gamma_1 a^3}{R^3}\frac{\mu E_0}{\hbar\varepsilon_{effs}}$. The Rabi frequency $\Omega(t)$ in Eq. (3) includes two parts, one is the electric field induced by the direct coupling between the SQD and the applied field (i.e., Ω_0), and the other is the electric field from MNP that is induced by the external applied field (i.e., Ω) [3, 12, 24]. The parameter G arises when the applied field polarizes the SQD, which in turn polarizes the MNP and then produces a field to interact with the SQD. G is responsible for the interaction between a MNP and SQD, and can be defined as [3]

$$G = \sum_{j=1}^{l} \frac{1}{4\pi\varepsilon_e} \frac{(j+1)^2\gamma_j a^{2j+1}\mu^2}{\hbar\varepsilon_{effs}R^{2j+4}}, \tag{4}$$

where $\varepsilon_{effs} = \frac{2\varepsilon_e+\varepsilon_s}{3\varepsilon_e}$ is the effective dielectric constant of SQD with ε_s the background dielectric constant of the semiconductor. $\gamma_j = \frac{\varepsilon_m(\omega)-\varepsilon_e}{\varepsilon_m(\omega)+(j+1)\varepsilon_e/j}$ $(j = 1, 2, 3...)$, and $s_a = 2$ when the applied field is parallel to the major axis (z) of the system. In addition, the items with different j are related to different order multipole polarization in MNP. In the following analysis, we will take $l = 10$ in our calculations, as we find that this is enough to obtain converging results [3].

#235144 - $15.00 USD Received 25 Feb 2015; revised 15 Apr 2015; accepted 3 May 2015; published 8 May 2015
© 2015 OSA

The dynamics of the interaction system can be described by the following effective nonlinear Bloch equations beyond the rotating-wave approximation (RWA):

$$\dot{S_1}(t) = -\omega_{10} S_2(t) - \frac{S_1(t)}{T_2}, \tag{5}$$

$$\dot{S_2}(t) = \omega_{10} S_1(t) - 2\left[\Omega_R(t) + G_R S_1(t) + G_I S_2(t)\right] S_3(t) - \frac{S_2(t)}{T_2}, \tag{6}$$

$$\dot{S_3}(t) = 2\left[\Omega_R(t) + G_R S_1(t) + G_I S_2(t)\right] S_2(t) - \frac{S_3(t)+1}{T_1}, \tag{7}$$

where $S_1(t) = \rho_{01} + \rho_{10}$ and $S_2(t) = i(\rho_{10} - \rho_{01})$ are, respectively, the mean real and imaginary parts of polarization, and $S_3(t) = \rho_{00} - \rho_{11}$ is the mean population inversion with ρ_{jj} the occupation probability. In the Eqs. (5)-(7), $\Omega_R(t)$ is the real part of the Rabi frequency $\Omega(t)$, G_I and G_R are the imaginary and real parts of the parameter G, respectively. Finally, the terms containing the population decay time T_1 and the dephasing time T_2 describe relaxation processes in the SQD and have been added phenomenologically in Eqs. (5)-(7). The relaxation times T_1 and T_2 are influenced by the presence of the MNP [30]. However, for the parameters that we use here the values of T_1 and T_2 do not change much in the frequency region of interest, and therefore will be considered constant. According to the previous papers concerning similar systems [2, 5, 8, 21, 24], the influence of the relaxation time ($T_1 \sim 0.8$ ns, $T_2 \sim 0.3$ ns) can be neglected owing to the extremely short pulse width of the few-cycle laser field in the present study.

As far as we know, no closed-form solution of the nonlinear differential Eqs. (5)-(7) exists for fields of arbitrary temporal profile in the present complex system. In order to investigate the dynamic response of the excitonic population inversion in this system, we employ the fourth-order Runge-Kutta algorithm approach for solving Eqs. (5)-(7) for a specific parameters $T_1 =$ 0.8 ns, $T_2 = 0.3$ ns, $\varepsilon_e = \varepsilon_0$, $a = 7.5$ nm, $\mu = 0.65e$ nm, $\hbar\omega_0 = 2.5$ eV, and $\varepsilon_s = 6\varepsilon_0$, with ε_0 the dielectric constant of the vacuum. These parameter values correspond to the typically CdSe-based quantum dots and have been used in various studies [1, 3, 6, 12, 15, 24, 29, 31]. For $\varepsilon_m(\omega)$ we use the experimental values for gold nanoparticle [32].

Our calculations can be performed for a wide range of pulse shapes and related parameters. In the following, we will show the representative results for Gaussian pulse train ($f(t) =$ $\exp(-(t-nt_0)^2/\tau^2)$) and hyperbolic secant pulse train ($\mathrm{sech}((t-nt_0)/\tau)$), respectively. Besides, the time-dependent phase of the pulse train is chosen as $\dot{\phi}(t) = \alpha \tanh[(t-nt_0)/\tau]$ with α the chirp rate. The chirp form is controlled by adjusting the parameters α. Due to the recent advancement of comb laser technology, it is highly likely that such a time-varying CEP can be achieved in the near future [33]. First of all, we present the effects of MNP on the incident few-cycle pulse train. Figures 2(a) and 2(b) show the plasmonic fields of different shape few-cycle pulse trains. The corresponding plasmonic field enhancement spectrum of the MNP for different interparticle distances, $R = 15$ nm, $R = 30$ nm, and $R = 80$ nm are shown as red solid, blue dashed and black dotted curves, respectively. These figures show that modifying the incident pulse train by the MNP has a direct consequence of enhancing the field for small interparticle distance. The maximum field enhancement exceeds 1.5 for the small interparticle distance $R = 15$ nm. Second, we plot the time evolution of the population inversion $S_3(t)$ induced by the corresponding plasmonic fields for different interparticle distances, as shown in Fig. 2(c) and 2(d). One can find that complete population inversion does not occur for the large interparticle distances, i.e., $R = 30$ nm and $R = 80$ nm. However, complete excitonic population inversion occurs for a small interparticle distance $R = 15$ nm. The distance-sensitive population inversion in Fig. 2(c) and 2(d) can readily be understood by perturbation theory [34]. The large enhancement of plasmonic field for small R induce more population transitions between the

#235144 - $15.00 USD Received 25 Feb 2015; revised 15 Apr 2015; accepted 3 May 2015; published 8 May 2015
© 2015 OSA

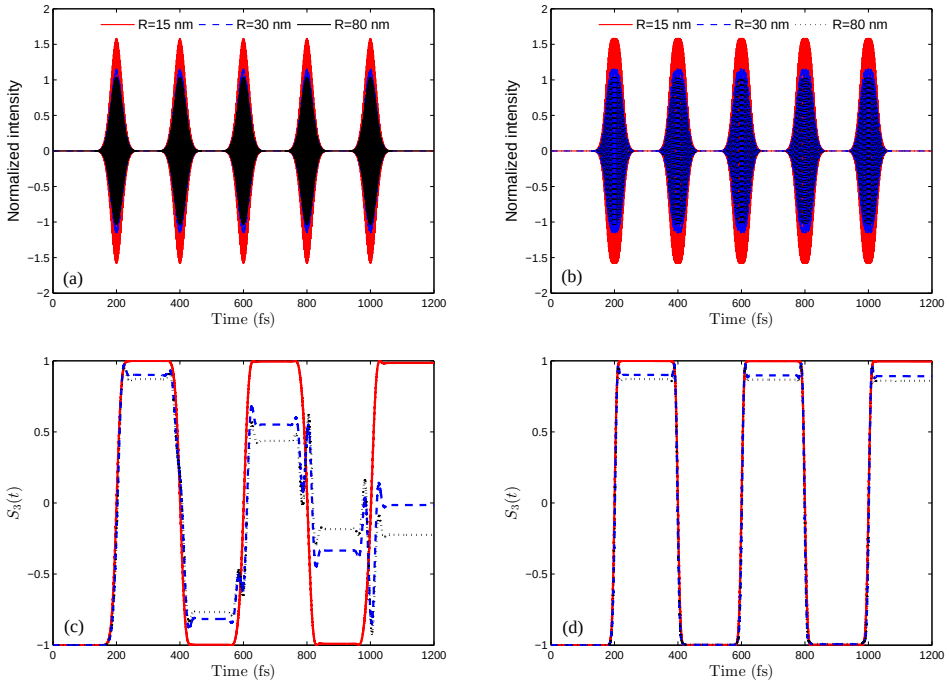

Fig. 2. The upper plots are the plasmonic fields inside the SQD for different interparticle distances, i.e., $R = 15$ nm (red solid curve), $R = 30$ nm (blue dashed curve), and $R = 80$ nm (black dotted curve), with (a) the incident Gaussian pulse train ($f(t) = \exp(-(t-nt_0)^2/\tau^2)$) and (b) the incident hyperbolic secant pulse train ($\mathrm{sech}((t-nt_0)/\tau)$). The lower plots are the the corresponding excitonic population inversion $S_3(t)$ from the numerical solution of Eqs. (5)-(7) for $R = 15$ nm (red solid curve), $R = 30$ nm (blue dashed curve), and $R = 80$ nm (black dotted curve), with (c) incident Gaussian pulse train and (d) incident hyperbolic secant pulse train. Other parameters of the pulse train are chosen as $N = 6$, $|\Omega_0| = 12$ meV, $\tau = 25$ fs, $t_0 = 200$ fs, and $\alpha = 5$.

ground and single-exciton state. Thus, one can easily conclude the enhancement of plasmonic field in vicinity of MNP plays an important role in controlling the excitonic population inversion dynamics. It can be also seen from Fig. 2(c) and 2(d) that the population are transferred to the single-exciton state during the interaction with the initial pulse ($n = 1$) in the pulse train for $R = 15$ nm. Subsequently, the population are transferred to the ground state after passing the second pulse ($n = 2$) in the pulse train. The holding time of population in the single-exciton state is nearly equal to the pulse repetition time $t_0 = 200$ fs. Remarkably, there is a steplike transition between the ground state and single-exciton state, from absorbing ($S_3 < 0$) to amplifying ($S_3 > 0$) as a function of the number of the pulses in the pulse train. For an odd number of the pulses, the complete inversion occurs. For an even number of the pulses, the population are transferred to the ground state. Direct comparison in Fig. 2(c) and 2(d) implies that population inversion is robust against the variation of pulse shape. Therefore, the excitonic population inversion of the SQD can be switched on and off by tuned the number of the pulses in the pulse train. And this optical switching provides an ultrafast and convenient way to achieve complete inversion.

We note that the above condition is not the only one that could control population inversion in the present SQD-MNP hybrid system. Based on the above Eqs. (5)-(7), we have calculated

#235144 - $15.00 USD Received 25 Feb 2015; revised 15 Apr 2015; accepted 3 May 2015; published 8 May 2015
© 2015 OSA

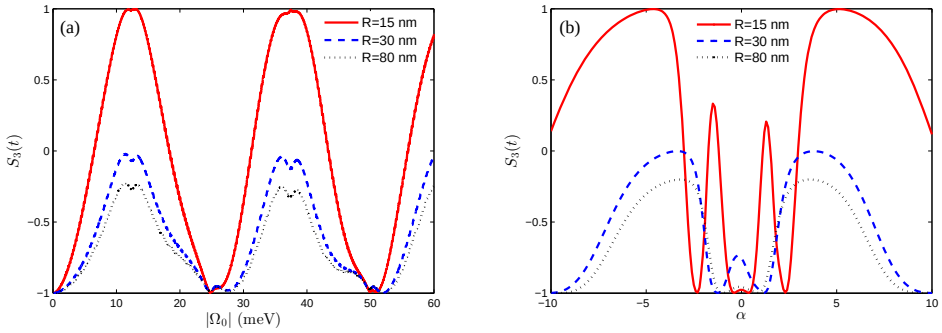

Fig. 3. The final excitonic population inversion S_3 at $t = 6t_0$ obtained from numerical solution of Eqs. (5)-(7) as a function of (a) input electric field amplitude $|\Omega_0|$ with $\alpha = 5$, with a Gaussian pulse train $N = 6$, for $R = 15$ nm (red solid curve), $R = 30$ nm (blue dashed curve), and $R = 80$ nm (black dotted curve), and (b) chirp rate α for the input electric field amplitude of the pulse train $|\Omega_0| = 12$ meV. Other parameters of the pulse train are chosen as $\tau = 25$ fs and $t_0 = 200$ fs.

numerically the final population inversion as a function of the input electric field amplitude of the pulse train $|\Omega_0|$ and chirp rate α after the passing of the Gaussian pulse train, as shown in Fig. 3. From Fig. 3(a), we can find that for chirp rate α up to $\alpha = 5$, high-efficiency population transfer from the ground state to the single-exciton state occurs for several values of $|\Omega_0|$, as long as $R = 15$ nm. Also, complete return to the initially occupied ground state can be found for several value $|\Omega_0|$ for small interparticle distance $R = 15$ nm. This figure shows a typical switching behavior that could be found in the present hybrid system. For the results of Fig. 3(a) the transfer process takes 1.2 ps. The effects of the interparticle distances on the maximum inversion are also shown in this figure. We note that for the large interparticle distances (i.e., $R = 30, 80$ nm) complete population transfer to the single-exciton state or complete population return to the ground state is not possible. In order to verify the robustness of the scheme for excitonic population inversion, we depict the evolution of the final inversion $S_3(t)$ against the variation of the chirp rate. The curve shows the population inversion is robust to the variation of the chirp rate. The complete population inversion can be achieved for $4.8 < |\alpha| < 5.2$. In other words, the switching behavior shown in Fig. 2 holds up to a wide region of the chirp rate α. In addition, the plots are symmetric and efficient population inversion can occur for both negative and positive values of the chirp rate. This behavior changes with the increase of the interparticle distances. For larger values of the interparticle distances, we find that complete population inversion does not occur. In this way, we might provide a scheme for obtaining a rough estimate of the interparticle distances between the MNP and SQD via probing the final population.

For a better insight into the effects of the input electric field amplitude of the pulse train and chirp rate on global behavior of the excitonic population inversion, the contour map of the final population inversion of $S_3(t)$ as the function of both $|\Omega_0|$ and α is shown in Fig. 4. It can be found from Fig. 4(a) there are a wide region of Ω_0 and α in which complete population inversion can be obtained under the condition $R = 15$ nm. However, if the interparticle distance increases, the maximum value of corresponding population transfer obtained will decrease. For $R = 80$, we plot in Fig. 4(b) the contour map of final population inversion $S_3(t)$ with the same other parameter settings. Compared with Fig. 4(a), the structure is qualitatively very similar, but the maximum value of population transfer becomes much smaller. Interesting enough, the influence of the distances on the excitonic population inversion depends strongly on the pulse

#235144 - $15.00 USD Received 25 Feb 2015; revised 15 Apr 2015; accepted 3 May 2015; published 8 May 2015
© 2015 OSA

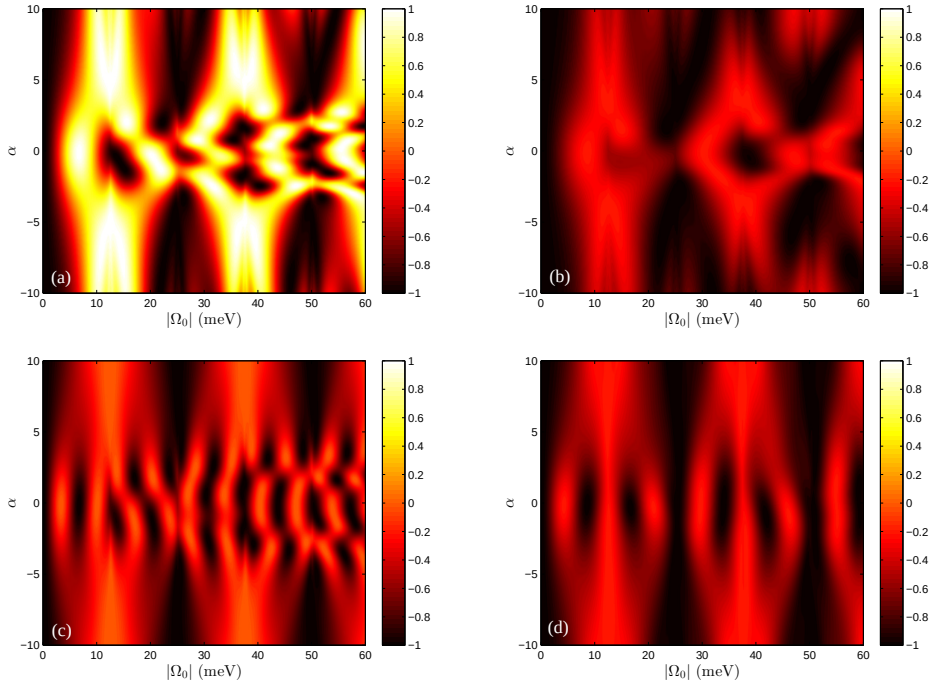

Fig. 4. Contour map of the final population $S_3(t)$ obtained from numerical solution of Eqs. (5)-(7) as a function of the input electric field amplitudes $|\Omega_0|$ and chirp rate α of the chirped Gaussian few-cycle pulse train for different interparticle distance R with fixed pulse duration $\tau = 25$ fs: (a) $R = 15$ nm; (b) $R = 80$ nm; with fixed pulse duration $\tau = 10$ fs: (c) $R = 15$ nm; (d) $R = 80$ nm. Other parameters are the same as Fig. 3.

duration τ. As an example, Figs. 4(c) and 4(d) show the contour map of the final population inversion of $S_3(t)$ as the function of both $|\Omega_0|$ and α for pulse duration $\tau = 10$ fs with different distances $R = 15$ nm and $R = 80$ nm. It can be found that the final excitonic population inversion is sensitive to the pulse duration. The effect of the pulse duration on the population inversion can be explained using the quasi-adiabatic following approximation [35]. As the pulse duration becomes shorter the enhanced effect of the plasmonic inside the SQD becomes less pronounced, which leads to the fact that the complete population inversion does not occur even for the small interparticle distance. In addition, the chirp rate α can modify the pulse duration, pulse shape as well as the pulse amplitude, thus the exciton population inversion depends on the chirp rate α, as illustrated in Fig. 3(b). This means that the pulse train for every R will not lead to complete excitonic population inversion for shorter pulse duration (see Figs. 4(c) and 4(d) for $\tau = 10$ fs). In other words, as the pulse duration becomes shorter, the influence of the plasmon effect weakens and smaller final populations are obtained.

An interesting effect is the influence of the input electric field amplitude of pulses on the final state of population inversion. We find that the dependence of final population inversion on the input electric field amplitude exhibits a typical switching behavior and this dependence is strongest for smaller interparticle distances. Moreover, the final population inversion is found to be sufficiently robust against the variation of the chirp rates. In order for maintaining clarity in the exposition, the present results were obtained in the context of symmetric pulse shapes. Actually, one can readily check that our results are robust with respect to the pulse shape.

#235144 - $15.00 USD Received 25 Feb 2015; revised 15 Apr 2015; accepted 3 May 2015; published 8 May 2015
© 2015 OSA

Of course, the present study was not exhaustive due to the enormous number of parameters involved. The typical example of these results shown in Fig. 4 shows that the complete population inversion can not maintain for shorter pulse duration. Finally, we should note that in the results presented above the pulse area is not a parameter that should get very specific values in order to achieve complete inversion, which is quite different from the Rabi solution of the optical Bloch equations for an atomic two-level system interacting with pulsed laser fields [36].

It is worth noting that our calculation performed for typical system parameters, i.e., those of CdSe SQD and Au nanoparticle complexes, demonstrated the ultrafast exciton population dynamics induced by the few-cycle pulse train. With the development of spectroscopy technology, the single-particle spectroscopy [37–39] could probably be used to realize these effects experimentally. The interaction between SQD and MNP depends on not only the pulse parameters and interparticle distance but also the orientation of the dipole moments of the two particles, therefore, switching can be achieved not only by the traditional control via the incident electric field amplitude and interparticle distance but also the polarization of the incident pulses. We believe that the modification of the surface plasmon on ultrafast excitonic population dynamics in our proposed hybrid system will also manifest itself in other quantum interference phenomena as well, and hence our study might open up an avenue to explore and utilize the these effects and could be exploited in real SQD-MNP hybrid as high speed optical modulators and switches.

In conclusion, we have studied the phenomenon of controllable ultrafast excitonic population dynamics in the hybrid system comprised of a SQD and a metal nanoparticle by utilizing the train of chirped few-cycle pulses. We have used the effective nonlinear Bloch equations for the description of the system dynamics. We present the numerical results for the case that the system interacts with the pulse train for Gaussian or hyperbolic secant envelope. Our findings showed that the excitonic population inversion can be modified for small interparticle distances due to the interaction between exciton and surface plasmon. We also showed that the time evolution of excitonic population inversion in the SQD exhibits a steplike transition between absorption and amplifying for small interparticle distance. These results suggest a straightforward method for measuring the interparticle distances from the final state of the inversion occur. This can be realized by injecting a probe beam in order to determine the state of the SQD. Probe amplification would indicate that the SQD was left in the single-exciton state, whereas probe absorption would indicate that the SQD was left in the ground state.

Acknowledgments

We appreciate useful discussions with Y. Wu. The research is supported in part by National Natural Science Foundation of China under Grant Nos. 11374050 and 61372102, by Qing Lan project of Jiangsu, and by the Fundamental Research Funds for the Central Universities under Grant No. 2242012R30011.

#235144 - $15.00 USD Received 25 Feb 2015; revised 15 Apr 2015; accepted 3 May 2015; published 8 May 2015
© 2015 OSA